

# Tobacco mutants with reduced microtubule dynamics are less susceptible to TMV

Maurice O. Ouko<sup>1</sup>, Adrian Sambade<sup>2</sup>, Katrin Brandner<sup>2</sup>, Annette Niehl<sup>2</sup>, Eduardo Peña<sup>2</sup>, Abdul Ahad<sup>3</sup>, Manfred Heinlein<sup>2</sup> and Peter Nick<sup>1,\*</sup>

<sup>1</sup>Botanical Institute 1, University of Karlsruhe, Kaiserstraße 2, D-76128 Karlsruhe, Germany,

<sup>2</sup>Institut de Biologie Moléculaire des Plantes du CNRS, Université de Strasbourg, 12 rue du Général Zimmer, 67084 Strasbourg Cedex, France, and

<sup>3</sup>Department of Botany, University of British Columbia, Vancouver, BC, Canada

Received 28 October 2009; revised 15 February 2010; accepted 17 February 2010; published online 25 March 2010.

\*For correspondence (fax +49 721 608 419; e-mail peter.nick@bio.uni-karlsruhe.de).

## SUMMARY

A panel of seven SR1 tobacco mutants (*ATER1* to *ATER7*) derived via T-DNA activation tagging and screening for resistance to a microtubule assembly inhibitor, ethyl phenyl carbamate, were used to study the role of microtubules during infection and spread of tobacco mosaic virus (TMV). In one of these lines, *ATER2*,  $\alpha$ -tubulin is shifted from the tyrosinylated into the detyrosinated form, and the microtubule plus-end marker GFP-EB1 moves significantly slower when expressed in the background of the *ATER2* mutant as compared with the SR1 wild type. The efficiency of cell-to-cell movement of TMV encoding GFP-tagged movement protein (MP-GFP) is reduced in *ATER2* accompanied by a reduced association of MP-GFP with plasmodesmata. This mutant is also more tolerant to viral infection as compared with the SR1 wild type, implying that reduced microtubule dynamics confer a comparative advantage in face of TMV infection.

**Keywords:** tobacco mosaic virus, microtubules, movement protein, *Nicotiana tabacum* SR1:nn cv. 'Petit Havana', activation tagging.

## INTRODUCTION

Evolutionary studies suggest that viruses exploit host cellular genes and pathways, adapting them for the viral life cycle (Citovsky, 1993; Koonin and Dolja, 1993; Ploubidou and Way, 2001; Worobey *et al.*, 2007). It is evident that the cytoskeleton as central element of motility represents a central target for this viral usurpation. In fact, many animal viruses spread through interaction with the microtubular cytoskeleton of the host (Greber and Way, 2006; Leopold and Pfister, 2006; Radtke *et al.*, 2006). The cellular function usurped here might be motor-driven transport of mRNA, which has been investigated in neurons, migrating fibroblasts, but also in polarizing yeast cells (for a recent review, see Martin and Ephrussi 2009). Signalling through specific RNA species is not limited to animals but is common in plants as well (Ruiz-Medrano *et al.*, 1999; for review see Lucas *et al.*, 2001). Actually, the first investigated example for transmissible signals that later turned out to be RNA has been the transport of morphogenetic signals from the nucleus into the hood-forming stalk in the green alga *Acetabularia* (Hämmerling, 1934). Based on the evolutionary conservation of actin and microtubules it is predicted that

plant viruses may use the cytoskeleton for propagation in a way similar to that observed for animal hosts.

When a virus is introduced into a plant, usually by mechanical means or by an insect vector, it is usually deposited in a few cells or even in a single cell. For successful systemic infection to occur, the virus has to move from the initially infected cell to adjacent cells and eventually through the rest of the plant. Viral spread in plants has long been considered to proceed in two distinct phases: slow movement from cell to cell occurring via the plasmodesmata and, subsequently, rapid distribution with the flow of photoassimilates in the phloem. Viral transport has been most intensively studied in the case of tobacco mosaic virus (TMV). The viral RNA of TMV moves from cell to cell by virtue of a virus-encoded movement protein (TMV-MP). The TMV-MP is observed in three characteristic patterns, punctate and larger aggregates along the endoplasmic reticulum, and colocalized with microtubules and plasmodesmata. The model to explain these patterns suggests that viral RNA/TMV-MP complexes assemble near the endoplasmic reticulum, probably anchored to microtubules,

and move then to the plasmodesmata by an ER-mediated mechanism that also involves microtubules (for a recent review see Heinlein, 2008).

Despite the involvement of microtubules in virus infection, little is known on the actual mechanisms of intracellular movement of viral components within the infected cells. There has been even a debate whether microtubules are actually involved at all (for instance Gillespie *et al.*, 2002 versus Seemanpillai *et al.*, 2006), and it has been proposed that the virus utilizes actin as transport system (Liu *et al.*, 2005; Wright *et al.*, 2007; Harries *et al.*, 2009). However, there is strong evidence that microtubules are important for the early events of viral movement (Boyko *et al.*, 2007), potentially in the release of mobile MP complexes from their assembly sites and subsequent displacement in the endoplasmic reticulum (Sambade *et al.*, 2008).

The interaction of the TMV-MP with microtubules may be based on molecular mimicry: a conserved motif has been identified in the TMV-MP that exhibits similarity to an  $\alpha$ -tubulin motif involved in lateral interactions of microtubule protofilaments suggesting that this conserved region mediates the association of MP with microtubules during infection. Viruses that display temperature-sensitive point mutations in this putative tubulin binding domain of the MP show reduced cell-to-cell spread and loss of microtubule association at the non-permissive temperature, suggesting that the spread of viral RNA is closely linked to the ability of MP to interact with microtubules (Boyko *et al.*, 2000b). Functional recovery of the viral movement function of MP at the permissive temperature correlates with the appearance of mobile MP-particles near linear tracks, and the subsequent reassociation of MP along microtubules (Boyko *et al.*, 2000a,b, 2007). This work was complemented by the demonstration that intramolecular complementation between different mutations in MP restored both the binding of MP to microtubules as well as the spread of infection (Boyko *et al.*, 2002), thus confirming that interactions between MP and microtubules are important for the cell-to-cell movement of the virus.

However, although these findings (Boyko *et al.*, 2002, 2007) confirm the significance of the interaction between MP and microtubules for the spread of viral infection, the specific role of microtubules in this process remains to be elucidated. There exist basically two possible mechanisms: (i) Microtubule serve as tracks for the translocation of viral RNA complexes from replication sites to plasmodesmata driven by molecular motors (Heinlein *et al.*, 1995; Zambryski, 1995; Carrington *et al.*, 1996; Aaziz *et al.*, 2001), (ii) Microtubules tether and release the infection particles from their assembly site or even move the MP particles along the ER by polymerization of tubulin heterodimers (Sambade *et al.*, 2008). This mechanism is supported by the observation that MP interacts with GFP-tagged Arabidopsis EB1a *in vivo* and *in vitro* (Brandner *et al.*, 2008) and the sensitivity

of MP-particle movement to inhibition of microtubule polymerization (Sambade *et al.*, 2009). During later stages of infection the MP accumulates on microtubules, which rather inhibits viral movement (Ashby *et al.*, 2006; Boyko *et al.*, 2007) and involves the recruitment of the MP-binding factor MPB2C (Kragler *et al.*, 2003; Curin *et al.*, 2007; Ruggenthaler *et al.*, 2009).

In order to discriminate between motor-driven and assembly-driven movement, we used tobacco mutant plants generated by T-DNA activation tagging. Mutants were selected for their tolerance to ethyl-*N*-phenylcarbamate (EPC), a compound that sequesters tubulin dimers and therefore eliminates microtubules depending on their innate turnover. As the mutant phenotype is expected to result from activation of the tagged genes, the tolerance of these plants to EPC is expected to be caused by reduced microtubular dynamics (Ahad *et al.*, 2003). If viral movement is brought about by a polymerization-dependent mechanism, it should be impaired in these mutants. We therefore analyzed the EPC tolerance in these *Activation-Tagged EPC-Resistant (ATER)* mutants in relation with their response to TMV. Using the mutant line *ATER2*, we demonstrate that reduced microtubule turnover significantly reduces the cell-to-cell transport of GFP-tagged TMV-MP and increases the tolerance to TMV suggesting a role of microtubule dynamics for viral movement.

## RESULTS

### Reduced EPC sensitivity and altered microtubule orientation in *ATER2*

To assess, to which extent microtubules in the *ATER2* differ from the SR1 wild-type line with respect to their sensitivity to EPC, we compared dose–response relations for growth over EPC concentration for both hypocotyls (in which growth is exclusively driven by cell expansion) versus roots (where growth depends on cell divisions in the meristem) in tobacco seedlings (Figure 1a). A clear dose dependency was observed with progressive inhibition of growth for increasing concentrations of EPC and roots being more sensitive as compared to hypocotyls. For both organs, *ATER2* was found to be more tolerant. At 30  $\mu\text{M}$  of EPC, there was no growth in the wild type, whereas the mutant still was able to grow, albeit at reduced rate. Similar results were obtained for the other *ATER* lines, with *ATER1*, *ATER2*, and *ATER5* being the most tolerant (data not shown). As the *ATER* plants are characterized by thicker, but shorter internodes, petioles and bushy inflorescences (Ahad *et al.*, 2003), we analyzed microtubule orientation in epidermal cells of petioles. In the SR1 wild type, most microtubules were oriented in a flat angle with the short cell axis (Figure 1b). In contrast, cells of the *ATER2* mutant were characterized by more steeply oblique or even longitudinal microtubules (Figure 1b).

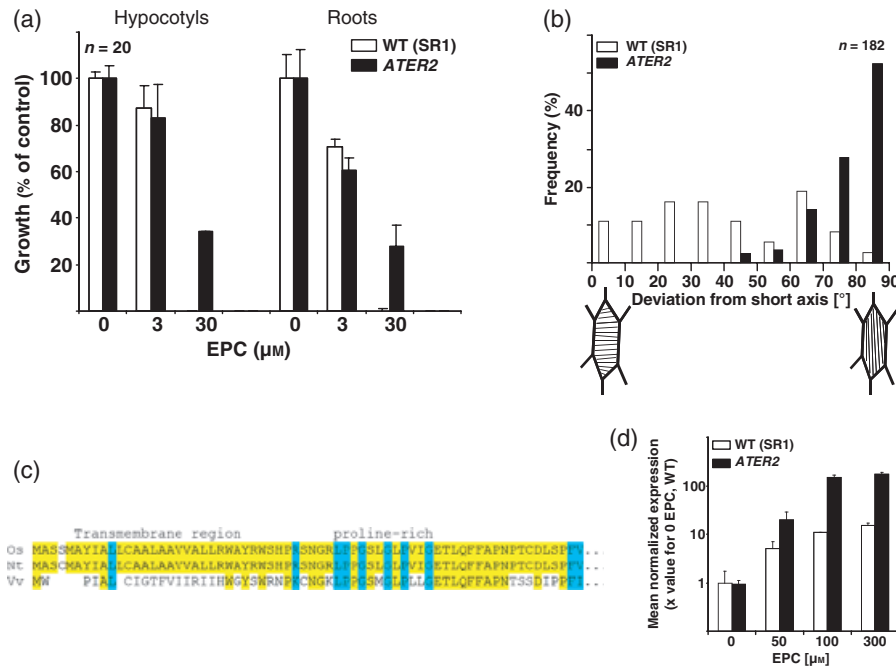


**Figure 1.** EPC sensitivity and activation tagging in the SR1 WT versus *ATER2*.

(a) Growth response of tobacco seedlings to the microtubule disrupting drug EPC. The *ATER2* mutant shows tolerance to high EPC concentrations.

(b) Orientation of cortical microtubules in epidermal cells SR1 wild type versus *ATER2*.

(c) Identification of the flanking sequence bordering the activation tag in *ATER2* as putative tobacco homologue of rice Cyp87A3. The alignment shows the N-terminal sequences of the Cyp87A3 cytochrome P450 from *Oryza sativa*, *Nicotiana tabacum* (*ATER2* flanking sequence), and *Vitis vinifera*.

(d) Induction of the *ATER2* transcript by EPC in the SR1 WT (white bars) and the *ATER2* line (black bars). Each value represents the mean of three independent experimental series with triplicates of each sample, error bars give  $s_e$ .

For *ATER2*, a fragment of the DNA downstream of the insertion site could be recovered by plasmid rescue. This fragment displayed homology with the N-terminus of a cytochrome P450 from rice (Cyp87A3; Chaban *et al.*, 2003), and, to a lesser extent to a cytochrome P450 from grapevine (Figure 1c). To assess, whether the tagged gene was activated, we followed the response of transcript abundance to EPC (Figure 1d). We observed that the tagged gene was induced by EPC in both wild type and mutant. However, the induction in the mutant was increased about 10-fold over that observed in the wild type. For the *ATER5* mutant, the recovered flanking sequences, so far, did not reveal any similarities to available sequences (data not shown).

### Reduced microtubule dynamics in *ATER2*

To test, whether the elevated EPC tolerance of the *ATER2* mutant is caused by a reduced global dynamics of microtubules, we assessed the relative abundance of the tyrosinylated versus the detyrosinated form of  $\alpha$ -tubulin by western blotting using antibodies discriminating the two modifications of  $\alpha$ -tubulin. Detyrosination of  $\alpha$ -tubulin is caused by a specific decarboxylase that prefers assembled microtubules over tubulin dimers, such that the proportion of detyrosinated  $\alpha$ -tubulin is a function of microtubule lifetime (Wiesler *et al.*, 2002). Compared with the respective signal of the wild type, the signal for tyrosinylated  $\alpha$ -tubulin

was virtually the same in the *ATER2* mutant (Figure 2a, tyr-Tub). In contrast, the signal for detyrosinated  $\alpha$ -tubulin was roughly doubled relative to the signal observed for the wild type (Figure 2a, detyr-Tub). This means that in the *ATER2* mutant the proportion of detyrosinated  $\alpha$ -tubulin is increased as compared to the SR1 wild type line suggesting differences in MT dynamics.

We measured microtubule dynamics by using the microtubule plus-end marker EB1a. A GFP-fusion construct of *AtEB1a* was transiently expressed in leaves of the wild type and the *ATER2* mutant. The *AtEB1a*-GFP visualizes comet-like structures that move along tracks and visualize the growing ends of microtubules (Chan *et al.*, 2003). The movement of these comets was more vivid upon transfection into the wild type (Figure 2b, left) as compared with the *ATER2* mutant (Figure 2b, right) and also in the *ATER5* mutant that was analyzed in parallel (data not shown). A quantification of comet movement using kymographing showed that microtubule growth in the mutant was reduced significantly by 15% as compared to the wild type (Figure 2c).

### Reduced cell-to-cell movement of TMV in *ATER2*

To assess whether the reduced microtubule dynamics in the *ATER2* mutant influenced the efficiency of cell-to-cell movement of TMV, we used TMV-MP-GFP5 (Boyko *et al.*,

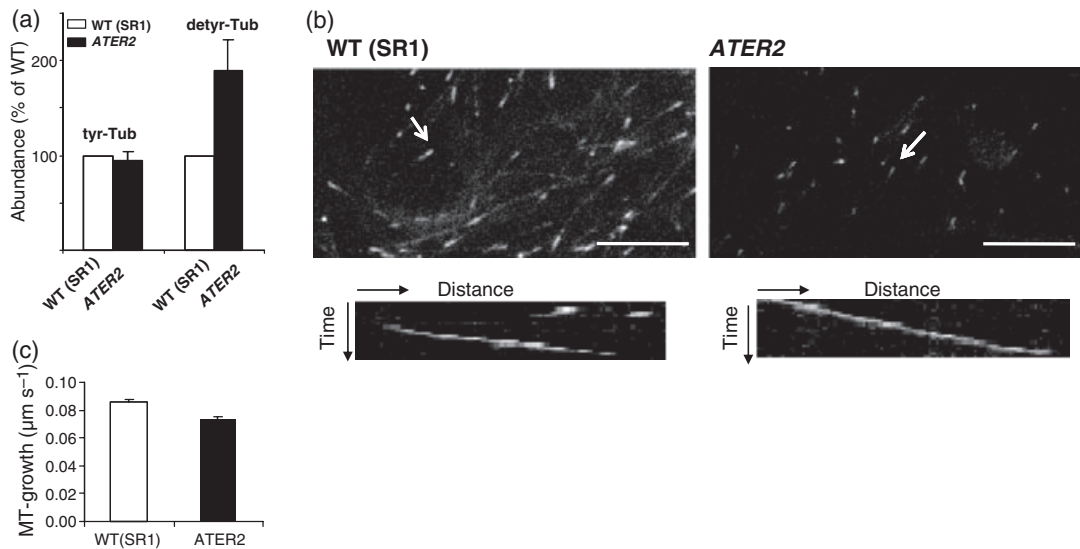


**Figure 2.** Microtubule dynamics in the SR1 WT versus *ATER2*.

(a) Abundance of tyrosinated and detyrosinated  $\alpha$ -tubulin in total protein extracts from leaves of the SR1 WT (white bars) and the *ATER2* mutant (black bars). Data represent mean values from five independent experimental series.

(b) Frames from a time-lapse series showing leaf epidermis of the SR1 WT and the *ATER2* mutant transiently expressing AteB1a-GFP. Arrows indicate the position of fluorescent comets representing the growing end of microtubules. Size bar corresponds to 10  $\mu\text{m}$ . The lower row show representative kymographs of individual comets.

(c) Quantification of AteB1a-GFP comet movement in leaf epidermis of the SR1 WT and the *ATER2* mutant. Values represent the mean from 40 individual kymographs, error bars give  $s_e$ .

2002), a TMV variant, in which the movement protein (MP) is tagged with GFP. A fluorescent halo around the inoculation sites on the leaves is indicative of successful inoculation and infection of tobacco plants with TMV-MP-GFP5 (Figure 3a). The expansion of the fluorescent infection site over time monitors the efficiency of TMV movement whereas the distance between the leading and trailing edges of the fluorescent halo mirror the accumulation and subsequent disappearance of MP-GFP5 (Figure 3a). In both, wild type and *ATER2* mutant, infection sites were observed to expand over time (Figure 3b) and the velocity of expansion could be measured by comparison of the individual infection sites at 5 and 7 days post infection (dpi). Interestingly, in *ATER2*, the distances from the centre of infection to both leading and trailing edges of the fluorescent halo were for both time points reduced by about 25% as compared with the SR1 wild type (Figure 3b). This means that at the same relative reduction of expansion, the (larger) distance of the leading edge suffers a stronger reduction in its absolute value as compared to the (smaller) distance of the trailing edge. Thus, the bandwidth (as distance between the leading and trailing edges) is expected to be reduced by the same relative value. This is exactly that what was observed. The bandwidth, although constant over time, was reduced by about 25%. Based on the expansion of the fluorescent halo over time, the virus spread was estimated to be 0.2 mm day<sup>-1</sup> in wild-type plants whereas the spread in *ATER2* plants was reduced to 0.15 mm day<sup>-1</sup> under the same conditions. Similar results

were obtained with the line *ATER5* plants that were tested in parallel (data not shown).

To test, whether the reduced viral spread was caused by reduced viral replication in the mutant background, we used two approaches: on the one hand, protoplasts from wildtype and *ATER2* were infected with TMV-MP:GFP or with wild-type TMV and viral genomic RNA was quantified by RT-PCR. The RT-PCR data do not show any indication for an effect of *ATER2* on virus replication; both positive and negative viral strands appear not to be affected (data not shown). To verify these findings, we used a second approach, and infected plants from wildtype, *ATER2*, and *ATER5* with TMV-GFP (a virus expressing free GFP). The growth of a number of individual infection sites was measured at different time points. At 9 dpi, the average sizes of infection sites of both *ATER2* and *ATER5* plants was significantly reduced (by about 15%) as compared with the wild type (Figure S1a). The viral RNA in those infection sites was quantified by RT-PCR 12 dpi. Again, there was no reduction in the amount of viral RNA in *ATER2* and *ATER5* as compared to wild type. In contrast, if at all, replication was slightly increased in the mutants as compared to the wildtype (Figure S1b). Both approaches indicated that the reduced viral spread in the mutants is not caused by a reduced viral replication.

In order to spread from cell to cell, the viral movement complexes have to be delivered to the plasmodesmata. Thus, plasmodesmata in infection sites are usually labelled with MP-GFP (Gillespie *et al.*, 2002; Heinlein *et al.*, 1998;

Kahn *et al.*, 1998; Kotlitzky *et al.*, 2001). We observed that, in the wild type, the walls of epidermal cells were labelled by MP-GFP (Figure 3c). This fluorescence of the cell walls appeared as duplicate spots in the focal plane or as a more diffuse background fluorescence above or below the focal plane. Similar duplicate spots have been observed for other plasmodesmatal proteins and could be explained by optical reflection across plant cell boundaries (Liu *et al.*, 2008). In *ATER2*, plasmodesmatal labelling by MP-GFP was significantly weaker. Moreover, diffuse fluorescence of the cell wall (originating from plasmodesmata situated outside the respective focal plane) was almost not detectable. A quantification of plasmodesmatal labelling showed a reduction by about a third in the *ATER2* mutant as compared with the SR1 wild type (Figure 3d), indicating that *ATER2* plants accumulate less MP-GFP in plasmodesmata.

The TMV-MP has been shown to associate with microtubules in *Nicotiana benthamiana* (Heinlein *et al.*, 1998; Boyko *et al.*, 2000a) and *Nicotiana tabacum* (Padgett *et al.*, 1996). To test microtubule-association in our *N. tabacum* plants we coexpressed MP-GFP with the microtubule marker RFP-MAP4-MBD (Van Damme *et al.*, 2004), and observed a close colocalization of the two signals (Figure 3e).

### Reduced susceptibility to TMV in *ATER2*

To determine whether the reduced microtubule dynamics in *ATER2* had an impact on the susceptibility to TMV infection, we mechanically inoculated plants of wild type and *ATER2* with wild-type TMV. Infected plants showed, following the formation of mosaic-like leaf chlorosis, a strong necrosis of infected tissues. This was observed in five independent series with three individual plants per line (Figure 3f) without specific features of a systemic hypersensitive response consistent with the lack of a functional N-gene in SR1 (Dinesh-Kumar *et al.*, 2000). The expression of symptoms was followed by scoring the frequency of necrotic leaves (Figure 3g). We observed that the *ATER2* mutant performed significantly better under viral infection with a 25% reduction of necrosis as compared to the wild type. Thus, the *ATER2* mutant is less susceptible to TMV and the reduction of susceptibility (about 25%) corresponds to the reduction in cell-to-cell movement of TMV-MP-GFP5 (compare Figure 3b,d,g). Similar results were obtained for *ATER5* (data not shown).

### DISCUSSION

It is still far from clear how ER-localized MP and MP:vRNA complexes actually move. They could be either pulled actively along stable microtubules by kinesins (motor-driven movement, Carrington *et al.*, 1996; McLean *et al.*, 1995) or could attach to dynamic microtubules and move forward through microtubule polymerization (nucleation-driven movement). As to be expected from the close interaction between microtubules and actin filaments (for a recent

review see Collings, 2008) there is also an influence of ER-associated actin filaments that has been discussed in detail elsewhere (Hofmann *et al.*, 2009; for recent reviews see Hofmann *et al.*, 2007; Sambade and Heinlein, 2009).

Microtubule nucleation-driven movement is supported by the observation that ectopic expression of the microtubule plus-end marker AtEB1a (visualized by fusion with GFP) reveals interaction with MP (Brandner *et al.*, 2008). Moreover, MP cannot only bind to assembled microtubules but also to tubulin dimers *in vitro* (Ferralli *et al.*, 2006) a precondition for movement through treadmilling. Recently, it has been demonstrated that plants in which the microtubule cytoskeleton is modified by overexpression of the microtubule-binding protein MPB2C show resistance against *oilseed rape mosaic virus*, a close relative of TMV (Ruggenthaler *et al.*, 2009). If MPB2C overexpression reduced microtubular dynamics, the observed viral resistance would support a model of polymerization-driven movement. However, it is not clear whether microtubule dynamics in this line is altered, although the phenotypes might be interpreted in this way. Moreover, since MPB2C can interact with MP directly (Kragler *et al.*, 2003), such resistance may be caused through MP sequestration rather than through dysfunctional microtubule activity.

To address the role of microtubule polymerization for viral movement, we used a tobacco mutant that had been generated by T-DNA activation tagging and selected for reduced microtubule polymerization monitored by an elevated tolerance to ethyl-*N*-phenylcarbamate (EPC), a drug that sequesters tubulin dimers and prevents them from being integrated into polymerizing microtubules (Mizuno and Suzuki, 1991) such that microtubules are eliminated dependent on their innate turnover (Ahad *et al.*, 2003).

Formally, the elevated EPC tolerance of the *ATER* lines (for *Activation Tagged EPC-Resistant*) could also be caused by reduced uptake or translocation of the inhibitor or by reduced affinity of tubulin for EPC. For instance, in mammalian cells it could be shown that mutations in the M-loop of  $\beta$ -tubulin resulted in resistance to microtubule disrupting drugs (Cabral *et al.*, 1986), and point mutations in  $\alpha$ -tubulin were shown to be responsible for resistance to microtubule-eliminating dinitroaniline herbicides (Anthony *et al.*, 1998). However, considering that the *ATER* mutants were developed via activation tagging, the scenario of an altered binding site is unlikely as any insertion of the tag into an exon would result in a knock-down of the gene function. Moreover, when we directly assessed the EPC affinity of tubulin isolated from *ATER2* by EPC-affinity chromatography (Wiesler *et al.*, 2002), we found the same affinities as for the SR1 wild type (data not shown). The *ATER2* mutant is also more resistant to oryzalin (that has a different binding site) and cold (AA and PN, Karlsruhe, Germany, unpublished results, and Ahad *et al.*, 2003), which speaks against a tolerance mechanism that is based on reduced uptake or

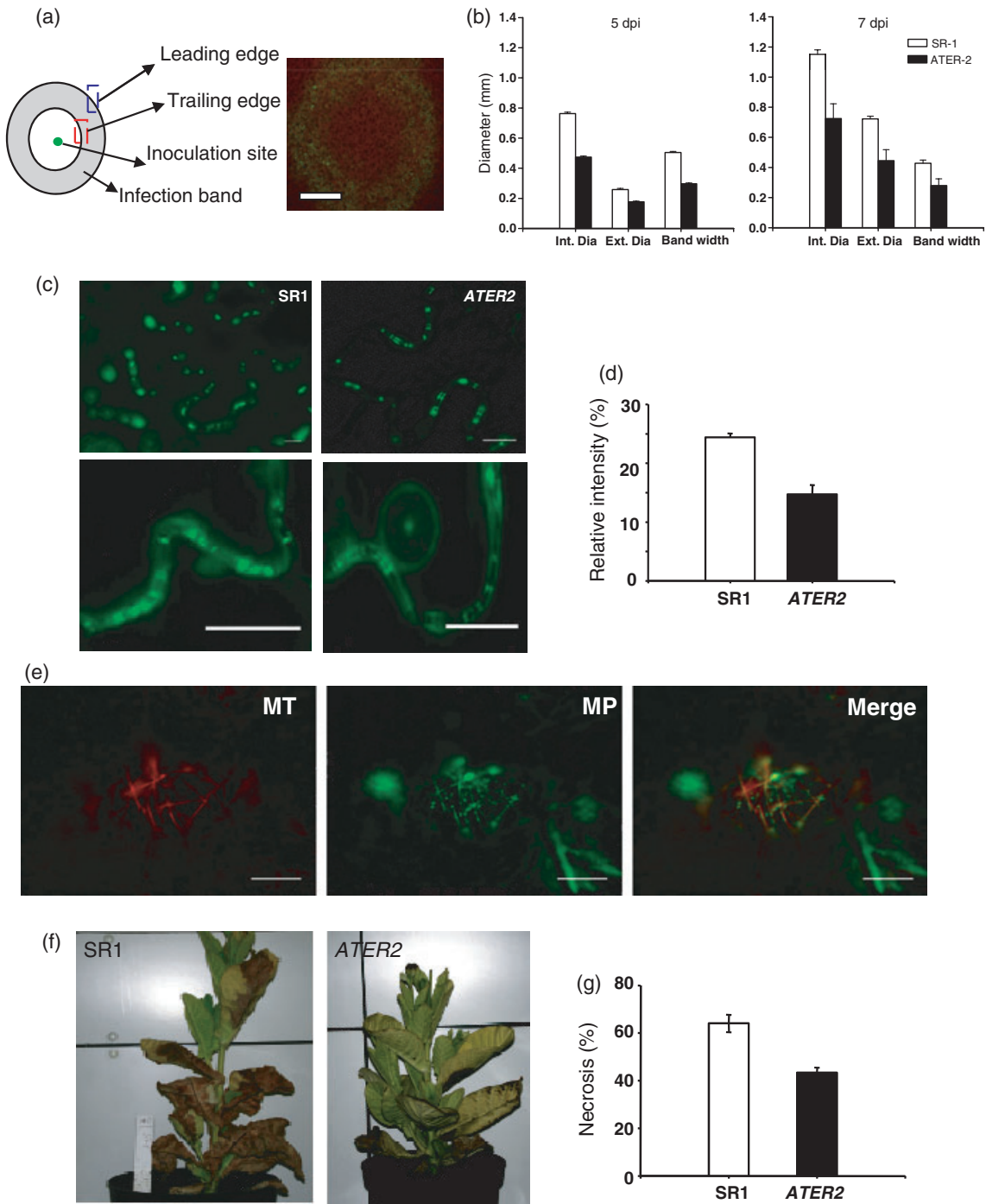


**Figure 3.** Quantification of TMV movement in the SR1 WT versus ATER2.

(a) Schematic representation and representative example of an infection focus following inoculation with TMV-MP-GFP. The band width is defined as the difference between the diameter of the internal band to that of the external band. Size bar 500  $\mu$ m.  
 (b) Band width, internal and external diameters of infection sites at 5 and 7 days post infection (dpi) in the SR1 WT versus ATER2. Values represent means from five independent series with three individual plants per line.  
 (c) Representative images and close-ups showing plasmodesmata labelling following infection with TMV-MP-GFP in the SR1 WT versus ATER2. Size bar 50  $\mu$ m.  
 (d) Quantification of cell-wall fluorescence in the SR1 WT versus ATER2. Values represent means from five independent series with three individual plants per line.  
 (e) Transient coexpression of the microtubule-binding domain of MAP4 in fusion with RFP (MT) and MP-GFP (MP) in the absence of viral infection in leaf epidermis of the SR1 WT. Scale bar 10  $\mu$ m.  
 (f) Representative images of SR1 WT versus ATER2 at 6 weeks after infection of the basal leaves with TMV.  
 (g) Proportion of necrotic leaves in the SR1 WT versus ATER2 at 6 weeks after infection with TMV. Values represent means from five independent series with three individual plants per line.

reduced affinity of tubulin for EPC. As expected from the reduced microtubule dynamics, longitudinal and steeply oblique microtubules were more frequent in *ATER2* as compared with the wild type, consistent with observations made in maize epidermis, where longitudinal microtubules were found to contain more deetyrosinated  $\alpha$ -tubulin than transverse microtubules (Wiesler *et al.*, 2002).

In *ATER2*, the activation tag is inserted into an intron of a putative cytochrome P450. The tagged gene was found to be induced by EPC, and this induction was upregulated tenfold in the *ATER2* mutant suggesting (although not providing final proof), that the mutant phenotype is caused by the activation of this cytochrome P450. To what extent this gene is regulated differentially during development, remains to be investigated. The recovered gene fragment reveals a very close relation with the rice Cyp87A3 (Chaban *et al.*, 2003). Interestingly, this putative rice homologue of the tagged tobacco gene had been isolated originally by fluorescent differential display comparing auxin-induced genes of wild type versus a mutant that had been recovered from a screen for EPC resistance (Wang and Nick, 1998). The biochemical activity of this gene is not understood so far, but it might act as regulator for the synthesis or activity of microtubule-associated proteins that control the dynamic equilibrium between assembly and disassembly of microtubules.

Three lines of evidence show that the *ATER2*-mutant is impaired in microtubule polymerization: (i) root and hypocotyl growth were found to proceed at higher concentrations of EPC as compared to the mutant, (ii) the ratio of deetyrosinated versus tyrosinylated  $\alpha$ -tubulin was doubled in *ATER2* indicative of an elevated activity of the tubulin-tyrosine decarboxylase, an enzyme that binds preferentially to assembled microtubules over non-assembled tubulin dimers such that its efficiency is positively correlated with the lifetime of microtubules (Skoufias and Wilson, 1998; Wiesler *et al.*, 2002), (iii) The mobility of the microtubule plus end marker EB1 in fusion with GFP, a direct reporter of microtubular polymerization activity *in vivo*, was found to be reduced to about a sixth upon expression in *ATER2* as compared to the SR1 wild type. From these three independent approaches we conclude that the treadmilling in *ATER2* is reduced significantly as compared to the SR1 wild type.

Based on the evidence for reduced microtubule turnover, it was possible to use *ATER2* as a tool to assess the role of reduced microtubule treadmilling in the movement of TMV. By following the progression of GFP-tagged TMV-MP in infected mutant versus wild-type plants, we found that cell-to-cell movement was reduced in the *ATER2* mutant. This reduced cell-to-cell movement was accompanied by a reduced expression of systemic disease symptoms. The wild type *N. tabacum* plants as well as *ATER2* exhibited an expanding fluorescent 'halo' around the sites of inoculation indicative of viral cell-to-cell movement. However, this movement was clearly reduced by about 25% in the mutant.

Thus, although the reduced microtubule turnover does not prevent viral infection *per se*, it does impair cell-to-cell movement. The participation of microtubules in viral movement was questioned by the argument that viral spread occurs at the leading edge of the infection site, whereas association of microtubules with the TMV-MP is observed at the trailing edge, i.e. during the later stages of infection (Padgett *et al.*, 1996; Gillespie *et al.*, 2002). Here we show that in the *ATER2* mutant not only the extension of the trailing edge of the infection foci (where microtubules are clearly decorated by MP), but also the extension of the leading edge is slowed down. This suggests that the association with microtubules is relevant already in the early stages of infection, before the microtubular association of the MP becomes detectable by fluorescence microscopy, which is consistent with a causative function of microtubules in viral movement. We further observed that the association of the tagged MP with plasmodesmata was reduced in *ATER2* as compared with the SR1 wild type, supporting a model, where the ER-mediated trafficking of viral replication complexes (VRCs) to PD depends on polymerizing microtubules. This is consistent with microtubule-associated MP particle movements observed in leading front cells and with the inhibition of their movements upon treatment with anti-microtubular drugs prior to the elimination of the microtubules themselves (Sambade *et al.*, 2008). Coexpression of MP-GFP with the MAP4-MBD microtubule marker in fusion with RFP showed a complete colocalization, confirming that neither viral replication nor virus-host interactions are necessary for the association of MP with microtubules, consistent with a direct binding of MP to microtubules *in vivo* and *in vitro* (Heinlein *et al.*, 1998; Ashby *et al.*, 2006; Ferralli *et al.*, 2006).

The SR1 line used as background for the mutants is susceptible to TMV and lacks a functional N resistance gene (Dinesh-Kumar *et al.*, 2000). Following TMV infection, the virus is capable of replication and systemic spread. The terminal necrosis observed as final stage of symptom expression is not caused by a systemic hypersensitive response. This necrotic response was much milder in the *ATER2* mutant as compared to the wild type, which was in good correlation with the reduced cell-to-cell movement observed with TMV-MP-GFP.

Based on the finding of the present study that TMV spreads slower in a mutant where microtubules are shown by several approaches to be less dynamic, we arrive at a scenario, where movement involves polymerizing microtubules and where reduced turnover such as in the *ATER2* mutant would increase the time to deliver or release their cargo. Thus, our findings support an involvement of nucleation-driven processes in virus movement. In contrast, a model for motor-driven processes would have predicted that the more stable microtubules in *ATER2* would drive viral transport more efficiently, which is not observed.

## EXPERIMENTAL PROCEDURES

### Plant material and EPC-resistance assay

The streptomycin-resistant, diploid tobacco line SR1 (*N. tabacum* cv. 'Petit Havana', Maliga *et al.*, 1973) and seven mutants generated in this background by T-DNA activation tagging (Ahad *et al.*, 2003) were used in this study. To assess the resistance against ethyl-*N*-phenylcarbamate (EPC), the seeds were first surface sterilized, then sown equidistantly on MS agar that contained varying concentrations of EPC. The plates were placed vertically, sealed with parafilm and incubated in the dark at 25°C. The length of hypocotyls and roots was measured at 14 days after sowing. Each data point represents the average from 20 individual seedlings.

### Immunostaining of microtubules

The cortical microtubule network was visualized by indirect immunofluorescence in epidermal cells of leaf petioles of wild type and *ATER* mutants as described in Nick *et al.* (1990) with modifications. Leaf petioles were harvested freshly from tobacco plants, these were then cut into 2-cm sections, placed in a 15-mm Falcon tube and fixed for 60 min in 3.7% (w/v) paraformaldehyde in microtubule stabilizing buffer (MSB: 50 mM PIPES, 2 mM EGTA, 2 mM MgSO<sub>4</sub>, 0.1% Triton X-100, pH 6.9), cells were washed in MSB three times for 10 min, and then, the epidermis was carefully peeled using a razor blade and fine tweezers; the epidermal strips were collected in MSB on a slide and covered with a perfusion chamber (Sigma-Aldrich, <http://www.sigmaaldrich.com/>). Unspecific reactions were blocked using 5% (w/v) bovine serum albumin in phosphate-buffered saline for 20 min. The epidermal strips were then incubated for 60 min at 37°C with a monoclonal mouse antibody directed against tyrosinated  $\alpha$ -tubulin (ATT; Sigma-Aldrich) diluted to a concentration of 1:100 in PBS. This was followed by an other wash step using PBS (3 times for 10 min). A secondary anti-mouse IgG conjugated with fluorescein-isothiocyanate (Sigma-Aldrich) antibody diluted to 1:25 with PBS was then used to incubate the strips for another 60 min at 37°C, the sections were then washed 5 times for 5 min, mounted immediately in PBS and observed using an Axiomager Z.1 microscope (Zeiss, <http://www.zeiss.com/>) equipped with an ApoTome microscope slider for optical sectioning and a cooled digital CCD camera (AxioCamMRm; Zeiss). The signal was recorded through the filter set 38 HE (excitation at 470 nm, beamsplitter at 495 nm and emission at 525 nm) using a  $\times 63$  plan apochromat oil-immersion objective. Images were processed and analyzed using the AxioVision (Rel. 4.5; Zeiss) software as described above. For publication, images were processed with respect to contrast and brightness using the Photoshop software (Adobe Systems, <http://www.adobe.com>). The orientation of microtubules was determined with respect to the short axis of the cell, i.e. 0° correspond to transverse, 90° to longitudinal microtubules. Frequency distributions over microtubule orientation were constructed over 56–85 samples per genotype.

### SDS-PAGE and western analysis

Total proteins were extracted from tobacco leaves, separated by SDS-PAGE and subjected to western blotting as described in Nick *et al.* (1995) with minor modifications. The monoclonal mouse antibody DM1A (Sigma-Aldrich) was used to probe for detyrosinated  $\alpha$ -tubulin (Wiesler *et al.*, 2002), whereas tyrosinated  $\alpha$ -tubulin was probed using the monoclonal mouse antibody ATT (Kreis, 1987). Both primary antibodies were diluted 1:300 in PBS. The signal was detected through a polyclonal secondary antibody against mouse IgG conjugated to alkaline phosphatase (Sigma-Aldrich) at a dilution of 1:2500 using standard protocols.

### Viral plasmids and inoculation

Infectious viral RNA coding for a tagged variant of TMV (TMV-MP-GFP5) was produced by *in-vitro* transcription of the plasmid pTf5nx2 (Boyko *et al.*, 2000c) using a MEGAscript T7 kit (Ambion Europe Ltd, <http://www.ambion.com>). The construct pTLW3 (Kubota *et al.*, 2003) harbouring the full-length cDNA copy of TMV-L RNA (Osman and Buck, 2003) was transcribed *in vitro* and used for the studies on long distance viral transport. Tobacco plants infected with this construct exhibit necrosis (Saito *et al.*, 1987). For *in-vitro* transcription the T7 MEGAscript<sup>®</sup> transcription kit (Applied Biosystems, <http://www.appliedbiosystems.com>) was used, the product restricted using Acc651 (NEB, <http://www.neb.com>), extracted by phenol/chloroform and precipitated by ethanol using standard protocols (Sambrook *et al.*, 1989). For inoculation, plants were used at 4–6 weeks after germination (corresponding to the six-leaf stage). Leaves measuring 3–5 cm in length were mechanically inoculated with the respective *in-vitro* transcripts. The leaf petiole was marked using a permanent marker for later identification of the inoculated leaves. The leaves were cleaned using distilled water. Two-thirds of the upper leaf surface were then dusted using silicon carbide powder (grain size 400; Sigma-Aldrich). The solution with the transcript was pipetted onto the dusted leaf, and gently spread over the leaf surface. The inoculated leaves were then washed with distilled water. Plants were then cultivated in the greenhouse in a 16:8 h (light: dark) cycle and at 18–25°C and 70% humidity. At 3, 5, 7 and 10 days post inoculation, the lower side of the leaf was examined for determination of successful infection. Infection spots were excised, vacuum-infiltrated with MS medium and examined under the microscope. For each experiment three plants of SR1, *ATER2* and *ATER5* plants were tested in five independent experimental series.

### Quantification of viral replication and spread

To assess viral spread, *N. tabacum* SR1, *ATER2* and *ATER5* plants were mechanically inoculated with infectious transcripts of TMV-GFP- $\Delta$ CP (Heinlein *et al.*, 1995). *In-vitro* transcripts were generated using the RiboMax T7 transcription kit following the instructions of the manufacturer (PROMEGA, <http://www.promega.com/>). Plants were maintained at 23°C with a 16 h photoperiod. Images of isolated infection sites (at least 14 per plant) were acquired using a Leica Z16 APOA microscope coupled to a Leica DFC360 FX camera controlled by LEICA APPLICATION SUITEV3 software. Single fluorescent infection sites were monitored over time and their size was measured using IMAGEJ software.

To assess viral replication, mesophyll protoplasts were prepared from plantlets 7 weeks after germination. In brief, the leaves were cut in fine stripes using a razor blade and directly submerged in protoplast solution (0.6 M sorbitol, 10 mM KCl, pH 5.8). Subsequently, the solution was replaced by protoplast solution containing 5 mg ml<sup>-1</sup> cellulase, 5 mg ml<sup>-1</sup> macerozyme and 5 mg ml<sup>-1</sup> BSA. Leaf-stripes were infiltrated in a vacuum desiccator for 30 min and subsequently incubated with gentle shaking for 3 h in the dark. After incubation, protoplasts were filtered through a 100  $\mu$ m filter and sedimented with buffer W5 (154 mM NaCl, 125 mM CaCl<sub>2</sub>, 5 mM KCl, 5 mM glucose, pH 5.8) for 5 min at 1000 *g*. After two washes in W5 buffer, protoplasts were resuspended in W5 buffer and stored on ice for 30 min. Then, protoplasts were washed twice in buffer MMM (15 mM MgCl<sub>2</sub>, 0.1% w/v MES, 0.6 M mannitol, pH 5.8), counted and resuspended to  $2 \times 10^6$  cells ml<sup>-1</sup> in MMM buffer. For PEG transformation, *in-vitro* transcribed TMV-MP-GFP5 RNA, or, alternatively, 50  $\mu$ g purified TMV virions were added and cells were incubated with an equal volume of 40% PEG containing

0.6 M mannitol and 100 mM CaCl<sub>2</sub> for 20 min, washed with MMM buffer and incubated in K3 buffer (Gamborg medium with B5 vitamins, 2,4D; 6-BAP; NAA, xylose and glucose, pH 5.7) for 24–96 h at 27°C in the dark. Integrity of protoplasts was monitored microscopically after incubation. To harvest, protoplasts were sedimented for 5 min at 1000 *g* and sediments were frozen in liquid nitrogen for subsequent extraction of RNA using the triazol kit (Sigma-Aldrich). 400 ng (in case of protoplasts at 96 h post infection), 600 ng (in case of protoplasts at 24 h post infection) or 1000 ng (in case of excised leaf material) were reverse-transcribed using either random hexamers, or TMV replicase specific forward primers for the generation of negative-strand specific cDNA, and MP-specific reverse primer for the generation of positive-strand specific cDNA. cDNA synthesis was conducted with Superscript III reverse transcriptase (Invitrogen, <http://www.invitrogen.com/>) according to the protocol of the manufacturer. The PCR was performed with primers amplifying a 205-bp fragment of the TMV genome, with the forward primer located in the replicase and the reverse primer located in the MP gene. The progress of the PCR amplification was checked after 25, 30 and 35 cycles, respectively, the annealing temperature was 60°C.

### Transient expression of EB1-GFP in tobacco leaves

*Agrobacterium tumefaciens* strain LBA 4404 (Life Technologies, <http://www.lifetechnologies.com>) transformed with a fusion construct of the microtubule end binding protein 1 (*AtEB1*) in fusion with green fluorescent protein (Chan *et al.*, 2003), was cultured as described in Sambade *et al.* (2008). The bacteria were resuspended to a final optical density (OD<sub>600</sub>) of 0.2 in water and used to infiltrate small leaves of 4-week-old tobacco plants that were still attached to the plant. The plants were then cultivated in the green house at 20–22°C and a 16 h L/8 h D photoperiod for 32 h. A 1 cm leaf disc was excised from the agro-infiltrated area, and syringe-infiltrated with Murashige-Skoog medium prior to microscopic inspection.

### Quantification of EB1-GFP movement

To quantify relocations of EB1a-GFP over time, excised plant tissues were observed with a Nikon TE2000 inverted microscope equipped for real-time imaging with a Roper CoolSnap digital charge-coupled device (CCD) camera, piezo-driven z-focus and a ×60 TIRF objective with 1.45 numerical aperture. GFP was excited with 460–500 nm and emission recorded between 510–560 nm. Metamorph (6.2r6) and ImageJ (1.38u) softwares were used for image acquisition, analysis and processing. Time-lapse images were acquired at intervals from 1 to 2.2 sec. Microtubule polymerization was analyzed in the time-lapse series and microtubule-life histories (kymographs) were plotted using ImageJ with the line tool and the 'Multyplekymograph' plug-in. 40 individual tracks were used for the quantification shown in Figure 2(c).

### Determination of MP-association with plasmodesmata

Fluorescence intensity at the cell wall indicative of plasmodesmata (Oparka *et al.*, 1997) was determined using the image analysis software ImageJ. Images of MP-GFP localized plasmodesmata were obtained with a fixed exposure, time and gain. The images were then converted from RGB to an 8-bit gray scale. After selecting the plasmodesmata as region of interest, average fluorescence intensity of the plasmodesmata subtracted by background fluorescence was used as measure for the association of MP-GFP with plasmodesmata. For each experiment three plants of SR1, *ATER2* and *ATER5* plants were tested in five independent experimental series.

### Plasmid rescue and expression analysis of the *ATER2* transcript

Fragments for sequences bordering the activation tag were obtained by plasmid rescue as described in Walden *et al.* (1995). Total RNA was isolated from the fully expanded 4th leaf of SR1 and *ATER2* plants that had been raised in a phytotron at a 16:8 h (light:dark) cycle at 25°C after treatment with variable concentrations (0–300 μM) of EPC for 2 h by using the RNeasy Plant Mini kit (Qiagen, <http://www.qiagen.com/>) extraction kit. Poly (dT) cDNA synthesis was performed with 1 μg total RNA in a 20 μl reaction mix using the iScript cDNA Synthesis Kit (BIO-RAD, <http://www.bio-rad.com/>) according to the protocol of the producer. Transcript levels were quantified using an iCycler iQ real-time PCR detection system (BIO-RAD) and the iQ™ SYBR® (BIO-RAD). PCR was carried out in 96-well microtiter plates in 25 μl reaction wells after heating to 95°C for 3 min, followed by 30 cycles of 30 sec at 95°C and 30 sec at 72°C, followed by a melting curve analysis from 54 to 95°C in steps of 0.5°C per step to test for potential bias through primer self-amplification (Norberg *et al.*, 2005). The statistical parameters for quantification were  $E > 0.95$ , and  $r^2 > 0.98$ , where E is the PCR efficiency and  $r^2$  corresponds to the correlation coefficient obtained with the standard curve. Three replicate assays were performed with independently isolated RNA and each sample was loaded in triplicates. The results were normalized to the expression of 18S ribosomal RNA.

### ACKNOWLEDGEMENTS

This project was funded by the German-French Procope Programme and a PhD fellowship of the State of Baden-Württemberg (Landesgraduiertenförderung) to MO, and supported by postdoctoral fellowships to K.B. (German Academic Exchange Service), and A.S. (CTBPDC/2204/015 and BPOSTDOC06/072; Generalidad Valenciana, Spain). We thank Professor Clive Lloyd, Dr Jordi Chan, The John Innes Centre, and the Biotechnology and Biological Sciences Research Council for providing the binary vector encoding AtEB1a:GFP. Mark Seemanpillai is acknowledged for support with inoculation and *in-vitro* transcription, Angelika Piernitzki for propagation of the *ATER* mutants.

### SUPPORTING INFORMATION

Additional Supporting Information may be found in the online version of this article:

**Figure S1.** Reduced viral spread in the mutants *ATER2* and *ATER5* is not caused by reduced viral replication.

Please note: As a service to our authors and readers, this journal provides supporting information supplied by the authors. Such materials are peer-reviewed and may be re-organized for online delivery, but are not copy-edited or typeset. Technical support issues arising from supporting information (other than missing files) should be addressed to the authors.

### REFERENCES

- Aaziz, R., Dinant, S. and Epel, B.L. (2001) The cytoskeleton and plasmodesmata: for better or for worse. *Trends Plant Sci.* **6**, 326–330.
- Ahad, A., Wolf, J. and Nick, P. (2003) Activation-tagged tobacco mutants that are tolerant to antimicrotubular herbicides are cross-resistant to chilling stress. *Transgenic Res.* **12**, 615–629.
- Anthony, R.G., Waldin, T.R., Ray, J.A., Bright, S.W.J. and Hussey, P.J. (1998) Herbicide resistance caused by spontaneous mutation of the cytoskeletal protein tubulin. *Nature*, **393**, 260–263.
- Ashby, J., Boutant, E., Seemanpillai, M., Groner, A., Sambade, A., Ritzenthaler, C. and Heinlein, M. (2006) Tobacco mosaic virus movement protein

- functions as a structural microtubule-associated protein. *J. Virol.* **80**, 8329–8344.
- Boyko, V., Ferralli, J., Ashby, J., Schellenbaum, P. and Heinlein, M. (2000a) Function of microtubules in intercellular transport of plant virus RNA. *Nat. Cell Biol.* **2**, 826–832.
- Boyko, V., Ferralli, J. and Heinlein, M. (2000b) Cell-to-cell movement of TMV RNA is temperature-dependent and corresponds to the association of movement protein with microtubules. *Plant J.* **22**, 315–325.
- Boyko, V., van der Laak, J., Ferralli, J., Suslova, E., Kwon, M.-O. and Heinlein, M. (2000c) Cellular targets of functional and dysfunctional mutants of tobacco mosaic virus movement protein fused to GFP. *J. Virol.* **74**, 11339–11346.
- Boyko, V., Ashby, J.A., Suslova, E., Ferralli, J., Sterthaus, O., Deom, C.M. and Heinlein, M. (2002) Intramolecular complementing mutations in tobacco mosaic virus movement protein confirm a role for microtubule association in viral RNA transport. *J. Virol.* **76**, 3974–3980.
- Boyko, V., Hu, Q., Seemanpillai, M., Ashby, J. and Heinlein, M. (2007) Validation of microtubule-associated tobacco mosaic virus RNA movement and involvement of microtubule-aligned particle trafficking. *Plant J.* **51**, 589–603.
- Brandner, K., Sambade, A., Boutant, E. et al. (2008) TMV movement protein interacts with GFP-tagged microtubule end-binding protein 1 (EB1). *Plant Physiol.* **147**, 611–623.
- Cabral, F.R., Brady, R.C. and Schibler, M.J. (1986) A mechanism of cellular resistance to drugs that interfere with microtubule assembly. *Ann. N.Y. Acad. Sci.* **466**, 745–756.
- Carrington, J.C., Kasschau, K.D., Mahajan, S.K. and Schaad, M.C. (1996) Cell-to-cell and long distance transport of viruses in plants. *Plant Cell*, **8**, 1669–1681.
- Chaban, C., Waller, F., Furuya, M. and Nick, P. (2003) Auxin responsiveness of a novel cytochrome P450 in rice coleoptiles. *Plant Physiol.* **133**, 2000–2009.
- Chan, J., Calder, G.M., Doonan, J.H. and Lloyd, C.W. (2003) EB1 reveals mobile microtubule nucleation sites in *Arabidopsis*. *Nat. Cell Biol.* **5**, 967–971.
- Citovsky, V. (1993) Probing plasmodesmal transport with plant viruses. *Plant Physiol.* **102**, 1071–1076.
- Collings, M. (2008) Crossed-wires: interactions and cross-talk between the microtubule and microfilament networks in plants. In *Plant Microtubules – Development and Flexibility* (Nick, P., ed.). Berlin Heidelberg New York: Springer, pp. 47–79.
- Curin, M., Ojangu, E.L., Trutnyeva, K., Ilau, B., Truve, E. and Waigmann, E. (2007) MPB2C, a microtubule-associated plant factor, is required for microtubular accumulation of tobacco mosaic virus movement protein in plants. *Plant Physiol.* **143**, 801–811.
- Dinesh-Kumar, S.P., Tham, W.H. and Baker, B.J. (2000) Structure–function analysis of the tobacco mosaic virus resistance gene N. *Proc. Natl. Acad. Sci. USA*, **97**, 14789–14794.
- Ferralli, J., Ashby, J., Fasler, M., Boyko, V. and Heinlein, M. (2006) Disruption of microtubule organization and centrosome function by expression of tobacco mosaic virus movement protein. *J. Virol.* **80**, 5807–5821.
- Gillespie, T., Boevink, P., Haupt, S., Roberts, A.G., Toth, R., Vantine, T., Chapman, S. and Oparka, K.J. (2002) Functional analysis of a DNA shuffled movement protein reveals that microtubules are dispensable for the cell-to-cell movement of tobacco mosaic virus. *Plant Cell*, **14**, 1207–1222.
- Greber, U.F. and Way, M. (2006) A superhighway to virus infection. *Cell*, **124**, 741–754.
- Hämmerling, J. (1934) Entwicklungsphysiologische und genetische Grundlagen der Formbildung bei der Schirmalge *Acetabularia*. *Naturwissenschaften*, **22**, 55–63.
- Harries, P.A., Park, J.W., Sasaki, N., Ballarda, K.D., Maule, A.J. and Nelson, R.S. (2009) Differing requirements for actin and myosin by plant viruses for sustained intercellular movement. *Proc. Natl. Acad. Sci. USA*, **106**, 17594–17599.
- Heinlein, M. (2008) Microtubules and viral movement. In *Plant Microtubules – Development and Flexibility* (Nick, P., ed.). Berlin Heidelberg New York: Springer, pp. 141–173.
- Heinlein, M., Epel, B.L., Padgett, H.S. and Beachy, R.N. (1995) Interaction of tobamovirus movement proteins with the plant cytoskeleton. *Science*, **270**, 1983–1985.
- Heinlein, M., Padgett, H.S., Gens, J.S., Pickard, B.G., Casper, S.J., Epel, B.L. and Beachy, R.N. (1998) Changing patterns of localization of the tobacco mosaic virus movement protein and replicase to the endoplasmic reticulum and microtubules during infection. *Plant Cell*, **10**, 1107–1120.
- Hofmann, H., Sambade, A. and Heinlein, M. (2007) Plasmodesmata and intercellular transport of viral RNA. *Biochem. Soc. Trans.* **35**, 142–145.
- Hofmann, C., Niehl, A., Sambade, A., Steinmetz, A. and Heinlein, M. (2009) Inhibition of TMV movement by expression of an actin-binding protein. *Plant Physiol.* doi:10.1104/pp.108.133827.
- Kahn, T.W., Lapidot, M., Heinlein, M., Reichel, C., Cooper, B., Gafny, R. and Beachy, R.N. (1998) Domain of the TMV movement protein involved in subcellular localization. *Plant J.* **15**, 15–25.
- Kotlizky, G., Katz, A., van der Laek, J., Boyko, V., Lapidot, M., Beachy, R.N., Heinlein, M. and Epel, B.L. (2001) A dysfunctional movement protein of Tobacco Mosaic virus interferes with targeting of wild type movement protein to microtubules. *Mol. Plant Microbe Interact.* **7**, 895–904.
- Koonin, E.V. and Dolja, V.V. (1993) Evolution and taxonomy of positive-strand RNA viruses. Implications of comparative analysis of amino acid sequences. *Crit. Rev. Biochem. Mol. Biol.* **28**, 375–430.
- Kragler, F., Curin, M., Trutnyeva, K., Gansch, A. and Waigmann, E. (2003) MPB2C, a microtubule-associated plant protein binds to and interferes with cell-to-cell transport of tobacco mosaic virus movement protein. *Plant Physiol.* **132**, 1870–1883.
- Kreis, T.E. (1987) Microtubules containing detyrosinated tubulin are less dynamic. *EMBO J.* **6**, 2597–2606.
- Kubota, K., Tsuda, S., Tamai, A. and Meshi, T. (2003) Tomato mosaic virus replication protein suppresses virus-targeted posttranscriptional gene silencing. *J. Virol.* **77**, 11016–11026.
- Leopold, P.L. and Pfister, K.K. (2006) Viral strategies for intracellular trafficking: motors and microtubules. *Traffic*, **7**, 516–523.
- Liu, J.Z., Blancaflor, E.B. and Nelson, R.S. (2005) The tobacco mosaic virus 126-kilodalton protein, a constituent of the virus replication complex, alone or within the complex aligns with and traffics along microfilaments. *Plant Physiol.* **138**, 1853–1865.
- Liu, D.Y.T., Kuhlmeier, B.T., Smith, P.M.C., Day, D.A., Faulkner, C.R. and Overall, R.L. (2008) Reflection across plant cell boundaries in confocal laser scanning microscopy. *J. Microsc.* **231**, 349–357.
- Lucas, W.J., Yoo, B.-C. and Kragler, F. (2001) RNA as a long-distance information macromolecule in plants. *Nat. Rev. Mol. Cell Biol.* **2**, 849–857.
- Maliga, P., Sz-Breznovits, A. and Marton, L. (1973) Streptomycin resistant plants from callus culture of haploid tobacco. *Nature New Biol.* **244**, 29–30.
- Martin, K.C. and Ephrussi, A. (2009) mRNA localization: gene expression in the spatial dimension. *Cell*, **136**, 719–730.
- McLean, B.G., Zupan, J. and Zambryski, P.C. (1995) Tobacco mosaic virus movement protein associates with the cytoskeleton in tobacco plants. *Plant Cell*, **7**, 2101–2114.
- Mizuno, K. and Suzuki, T. (1991) Effects of anti-microtubule drugs on *in vitro* polymerization of tubulin from mung bean. *Bot. Mag. Tokyo*, **103**, 435–448.
- Nick, P., Bergfeld, R., Schäfer, E. and Schopfer, P. (1990) Unilateral reorientation of microtubules at the outer epidermal wall during photo- and gravitropic curvature of maize coleoptiles and sunflower hypocotyls. *Planta*, **181**, 162–168.
- Nick, P., Lambert, A.M. and Vantard, M. (1995) A microtubule-associated protein in maize is expressed during phytochrome-induced cell elongation. *Plant J.* **8**, 835–844.
- Norberg, M., Holmlund, M. and Nilsson, O. (2005) The BLADE ON PETIOLE genes act redundantly to control growth and development of lateral organs. *Development*, **132**, 2203–2213.
- Oparka, K.J., Prior, D.A.M., Santa Cruz, S., Padgett, H.S. and Beachy, R.N. (1997) Gating of epidermal plasmodesmata is restricted to the leading edge of expanding infection sites of Tobacco mosaic virus. *Plant J.* **12**, 781–789.
- Osman, T.A.M. and Buck, K.W. (2003) Identification of a region of the tobacco mosaic virus 126- and 183-kilodalton replication proteins which binds specifically to the viral 3'-terminal tRNA-like structure. *J. Virology*, **77**, 8669–8675.
- Padgett, H.S., Epel, B.L., Kahn, T.W., Heinlein, M., Watanabe, Y. and Beachy, R.N. (1996) Distribution of tobamovirus movement protein in infected cells and implications for cell-to-cell spread of infection. *Plant J.* **10**, 1079–1088.
- Ploubidou, A. and Way, M. (2001) Viral transport and the cytoskeleton. *Curr. Opin. Cell Biol.* **13**, 97–105.

- Radtke, K., Dohner, K. and Sodeik, B.** (2006) Viral interactions with the cytoskeleton: a hitchhiker's guide to the cell. *Cell Microbiol.* **8**, 387–400.
- Ruggenthaler, P., Fichtenbauer, D., Krasensky, J., Jonak, C. and Waigmann, E.** (2009) Microtubule-associated protein AtMPB2C plays a role in organization of cortical microtubules, stomata patterning, and tobamovirus infectivity. *Plant Physiol.* **149**, 1354–1365.
- Ruiz-Medrano, R., Xoconostle-Cázares, B. and Lucas, W.L.** (1999) Phloem long-distance transport of CmNACP mRNA: implications for supracellular regulation in plants. *Development*, **126**, 4405–4419.
- Saito, T., Meshi, T., Takamatsu, N. and Okada, Y.** (1987) Coat protein gene sequence of tobacco mosaic virus encodes a host response determinant. *Proc. Natl Acad. Sci. USA*, **84**, 6074–6077.
- Sambade, A. and Heinlein, M.** (2009) Approaching the cellular mechanism that supports the intercellular spread of tobacco mosaic virus. *Plant Signal. Behav.* **4**, 35–38.
- Sambade, A., Brandner, K., Hofmann, C., Seemanpillai, M., Mutterer, J. and Heinlein, M.** (2008) Transport of TMV movement protein particles associated with the targeting of RNA to plasmodesmata. *Traffic*, **9**, 2073–2088.
- Sambrook, J., Fritsch, E.F. and Maniatis, T.** (1989) *Molecular Cloning: A Laboratory Manual*, 2nd edn. Cold Spring Harbor: Cold Spring Harbor Laboratory Press.
- Seemanpillai, M., Elamawi, R., Ritzenthaler, C. and Heinlein, M.** (2006) Challenging the role of microtubules in tobacco mosaic virus movement by drug treatments is disputable. *J. Virol.* **80**, 6712–6715.
- Skoufias, D.A. and Wilson, L.** (1998) Assembly and colchicine binding characteristics of tubulin with maximally tyrosinated and detyrosinated alpha tubulins. *Arch. Biochem. Biophys.* **351**, 115–122.
- Van Damme, D., Van Poucke, K., Boutant, E., Ritzenthaler, C., Inze, D. and Geelen, D.** (2004) In vivo dynamics and differential microtubule-binding activities of MAP65 proteins. *Plant Physiol.* **136**, 3956–3967.
- Walden, R., Fritze, K. and Harling, H.** (1995) Induction of signal transduction pathways through promoter activation. *Methods Cell Biol.* **49**, 455–469.
- Wang, Q.-Y. and Nick, P.** (1998) The auxin response of actin is altered in the rice mutant *Yin-Yang*. *Protoplasma*, **204**, 22–33.
- Wiesler, B., Wang, Q.Y. and Nick, P.** (2002) The stability of cortical microtubules depends on their orientation. *Plant J.* **32**, 1023–1032.
- Worobey, M., Bjork, A. and Wertheim, J.O.** (2007) Point, counterpoint: the evolution of pathogenic viruses and their human hosts. *Annu. Rev. Ecol. Syst.* **38**, 515–540.
- Wright, K.M., Wood, N.T., Roberts, A.G., Chapman, S., Boevink, P., MacKenzie, K.M. and Oparka, K.J.** (2007) Targeting of TMV movement protein to plasmodesmata requires the actin/ER network. Evidence from FRAP. *Traffic*, **8**, 21–31.
- Zambryski, P.** (1995) Plasmodesmata: plant channels for molecules on the move. *Science*, **270**, 1943–1944.